5676 *Macromolecules* **2009**, *42*, 5676–5683
DOI: 10.1021/ma9008719

Macromolecules
ARTICLE

Temperature Dependence of the Linear Steady-State Shear Compliance of Linear and Long-Chain Branched Polyethylenes

Julia A. Resch, Florian J. Stadler,† Joachim Kaschta, and Helmut Münstedt*

Institute of Polymer Materials, Friedrich-Alexander-University Erlangen-Nürnberg, Martensstrasse 7, D-91058 Erlangen, Germany. †*Present address: Unité de Physique et de Chimie des Hauts Polymères, Université catholique de Louvain, Croix du Sud, 1, B-1348 Louvain-la-Neuve, Belgium.*

Received April 21, 2009; Revised Manuscript Received June 2, 2009

ABSTRACT: The linear steady-state shear compliances J_e^0 of two linear short-chain branched metallocene-catalyzed polyethylenes (mLLDPE), two long-chain branched metallocene-catalyzed polyethylenes (LCB-mLLDPE), and two classical low density polyethylenes (LDPE) were determined in creep-recovery tests in shear between 130 and 190 °C. In order to investigate the dependence of J_e^0 on the molecular structure the polyethylenes were characterized by high-temperature size-exclusion chromatography coupled with a multiangle laser light scattering device (SEC−MALLS). For the linear mLLDPE the lowest J_e^0 independent of temperature were observed. For the LCB-mLLDPE having similar polydispersities as the linear mLLDPE not only an increase of J_e^0 by about 1 order of magnitude compared to the linear mLLDPE but also a significant decrease in J_e^0 with increasing temperature was found. For the LDPE possessing long-chain branches as well as higher polydispersities, the highest J_e^0 values were detected, which were also temperature dependent. For the LDPE, the decrease of J_e^0 with increasing temperature is less pronounced than for the LCB-mLLDPE. However, for both material types the temperature dependence of J_e^0 is much stronger than expected from the rubber elastic theory.

Introduction

Although the elastic behavior of polymer melts as e.g. the extrudate swell in extrusion is of great importance for processing it is not as extensively investigated as the viscous behavior. One reason for this fact is that well-defined elastic properties are not easy to determine. The extrudate swell which is experimentally not too difficult to obtain in most cases, however, is a nonlinear quantity caused by both shear and extensional deformation. Therefore, in this paper elastic properties under well-defined shear in the linear viscoelastic range are investigated. Creep-recovery experiments allow the determination of both the viscous part of the deformation characterized by the zero-shear rate viscosity η_0 and the elastic part described by the linear steady-state shear compliance J_e^0. Creep-recovery experiments are not used as frequently as other rheological tests in shear (dynamic-mechanical, stressing, or relaxation experiments). But they are a very suitable method for measuring J_e^0, as experimental access to long retardation times can more easily be obtained with these tests than in dynamic-mechanical experiments.

The linear steady-state compliance J_e^0 of a material depends on a number of molecular parameters. From the literature, it is known that for linear monodisperse polymers above the critical molar mass M_c, being 5.5 times the entanglement molar mass M_e ($M_c = 5.5\ M_e$), J_e^0 is molar mass independent.[1−3] Values on the order of 10^{-6}−10^{-5} Pa^{-1} are given. For commercial PMMA samples of very similar molar mass distributions J_e^0 data independent of the molar mass were observed.[4] However, J_e^0 increases distinctly with broadening of the molar mass distribution (MMD). This effect was thoroughly investigated for bi- and trimodal blends of linear nearly monodisperse polymers. It was shown for several polymers like PS[5−7] and polyisobutylene[8] that the presence of a high molar mass component in a blend increases J_e^0 significantly. J_e^0 as a function of the concentration of the high molar mass component exhibits a maximum at low amounts. Pechhold et al.[8] investigated blends of polyisobutylenes whose high molar mass component was 12.5 times higher in molar mass than that of the matrix. For these blends they report a maximum in J_e^0 100 times larger than J_e^0 of the blend partners. Graessley and Struchlinski[9] observed a similar behavior for blends of monodisperse polybutadienes. A broader molar mass distribution ($M_w/M_n > 2$) typical of many commercially available products increases J_e^0 as well. Data of Gabriel and Münstedt[10] on mLLDPE and mHDPE with a similar polydispersity ($M_w/M_n \approx 2$) and comparable M_w showed an increase in J_e^0 of about a factor of 30 compared to the narrowly distributed polybutadienes which can be regarded as model polymers for short-chain branched polyethylenes as they have a similar entanglement molar mass M_e.

The introduction of long-chain branches (LCB) increases J_e^0 as well.[10−18] J_e^0 of the long-chain branched materials proved to be higher by a factor of about 10 to 100 compared to their linear counterparts.[2,3,19,20]

For long-chain branched polymers, however, no comprehensive studies have been carried out concerning the influence of molar mass, branching architecture, or temperature on J_e^0, because of the lack of products of defined molar mass distributions and branching topographies. For polystyrenes with defined branching structures (stars, H-shaped polymers, combs) an increase of J_e^0 with increasing molar mass M_w was observed for a broad range of molar masses.[12,14,20]

For polyethylenes, the situation concerning the lack of defined products improved with the availability of metallocene-catalyzed products in the last years. Investigations on commercially available polyethylenes indicated that J_e^0 of LCB-mLLDPE is higher

*To whom correspondence should be addressed: Telephone: +49-9131-852-8593. Fax: +49-9131-852-8321. E-mail: polymer@ww.uni-erlangen.de.

 Published on Web 06/17/2009

Table 1. Molecular and Rheological Characteristics

material	M_w [kg/mol]	M_w/M_n	comonomer	T_m [°C]	η_0 (T = 150 °C) [Pa s]	η_0/η_0^{lin}	LCB_{Rheo}	LCB_{SEC}
L 6−2	111	2.5	hexene	119	15 500	1.2	none	none
L 6−4	124	2.9	hexene	120	16 400	0.8	none	none
LB 1	100	2.4	octene	102	33 100	3.7	starlike	little
LB 4	91	2.4	octene	106	45 400	7.1	starlike	little
LDPE 1	377	18		110	481 300	0.5	treelike	very high
LDPE 4	217	14		109	60 700	0.4	treelike	very high

by approximately 1 order of magnitude compared to linear mLLDPE.[21] Despite the broader molar mass distribution of LDPE J_e^0 was found to be similar or only slightly higher than for the LCB-mLLDPE. This finding was explained by differences in their branching functionalities.[10,15,16,21]

The temperature dependence of the linear steady-state compliance J_e^0 has rarely been investigated for polyethylene melts of different molecular structure. For linear and short-chain branched melts J_e^0 was found to be independent of the temperature or directly proportional to the absolute temperature T; i.e., they are only very slightly temperature dependent.[1]

The temperature dependence of viscoelastic properties of polyethylenes of different structures using $G'(\omega)$ and $G''(\omega)$ has been investigated but is not fully understood, yet. For LCB-mLLDPE a thermorheological complexity was frequently reported[22−24] but the answer on the question how such a behavior is reflected by the elasticity of polyethylenes of various molecular structures was not given. Creep-recovery experiments are a promising tool to tackle this open field.

Materials and Methods

Materials. In this study three different classes of polyethylenes (mLLDPE, LCB-mLLDPE, and LDPE) are investigated. Some of their fundamental data are given in Table 1. L 6−2 and L 6−4 are linear hexene-mLLDPE from Basell and Exxon, respectively. All materials were stabilized by 0.5 wt % Irgafos 168 and 0.5 wt % Irganox 1010 (Ciba AG, Basel, Switzerland).

Thermal and Molecular Characterization. The melting point was determined by DSC (TA Instruments DSC 2920) from the second heating run. The heating and cooling rates applied were 10 K/min.

Molar mass measurements were carried out by means of a high-temperature size-exclusion chromatograph (PL 220, Varian Inc.) equipped with a refractive index (RI) and an infrared detector (PolyChar, IR4). All measurements were performed using Shodex columns (UT806 M and UT807) at 140 °C in 1,2,4-trichlorobenzene (TCB) as the solvent. The high temperature SEC was coupled with a multiangle laser light scattering (MALLS) apparatus (Wyatt, DAWN EOS). Experimental details of the SEC−MALLS setup and the measuring conditions were previously published elsewhere.[25]

Rheology. For determining the linear steady-state compliance J_e^0 special requirements concerning measuring equipment and experimental practice are essential. Rheometers with low friction bearings and, thus, very little residual torques are necessary to conduct creep-recovery experiments with sufficient accuracy.[26] Concerning the experiment, it has to be ensured that the measurements are conducted in the linear viscoelastic regime and that the steady state is reached in the preceding creep and the recovery test.

Classically, creep-recovery tests used to be performed by individually constructed rheometers with a magnetic bearing;[27,28] their residual torque is very low and they are nearly friction free. The air bearings of the latest generation of commercially available rheometers also proved to be suitable for conducting creep-recovery tests within a certain accuracy limit.[18,29] A further improvement is achieved by the first commercial magnetic bearing rheometer, the TA Instruments AR-G2, which is used in this work.

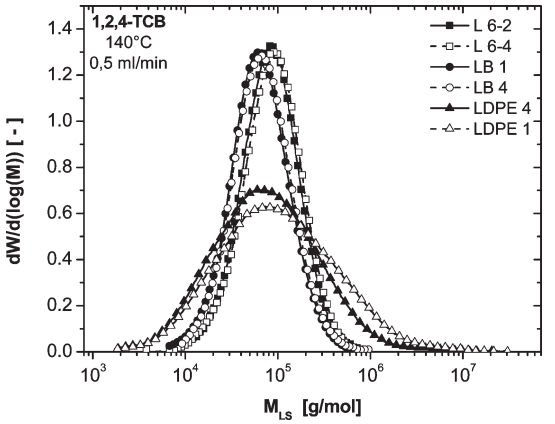

Figure 1. Molar mass distribution of the polyethylenes investigated.

The rheological tests were carried out in a nitrogen atmosphere using a 25 mm parallel-plate geometry. Creep and recovery tests were performed in the linear viscoelastic regime at stresses between 2 and 30 Pa. On each sample a frequency sweep (from ω = 628 to 0.01 s^{-1}) was conducted prior to the beginning and after the creep-recovery measurements to investigate the thermal stability during the test.

The samples were prepared in a hot press at 180 °C under vacuum. After the sample was loaded, a conditioning time of 10−45 min, depending on the elasticity of the sample, was applied to allow the normal forces in the melt to relax. Also between the initial frequency sweep and the following creep-recovery experiment this waiting time was applied.[30] Furthermore, a correction for residual torques has to be applied, in particular, if the recoverable part is low.[26]

Results

SEC−MALLS. The polyethylenes were characterized with respect to their absolute molar mass distribution by size-exclusion chromatography (SEC) coupled with multiangle laser light scattering (MALLS). The molar mass distributions are displayed in Figure 1. The corresponding molar mass averages are collected in Table 1. While the polymers synthesized using metallocene catalysts (L 6−2, L 6−4, LB 1, and LB 4) show similar narrow molar mass distributions for slightly different molar mass averages, broad distributions with a pronounced high molar mass tail are found in the case of the LDPE products.

The different topographies of the polymers show up in Figure 2 where the expected value of the square of the radius of gyration $\langle r_g^2 \rangle$ is plotted as a function of the absolute molar masses of the SEC-slices. The linear products L 6−2 and L 6−4 (not shown for reasons of clarity) come to lie on a straight line of a double logarithmic slope of 1.172 which corresponds to the exponent a = 0.586 in the scaling law

$$\langle r_g^2 \rangle^{0.5} = K M_{LS}^{a} \quad (1)$$

The values of the exponent as well as of the prefactor K of 0.024 (for $\langle r_g^2 \rangle^{0.5}$ in nm and M in g/mol) are in good agreement with the data published in the literature.[31]

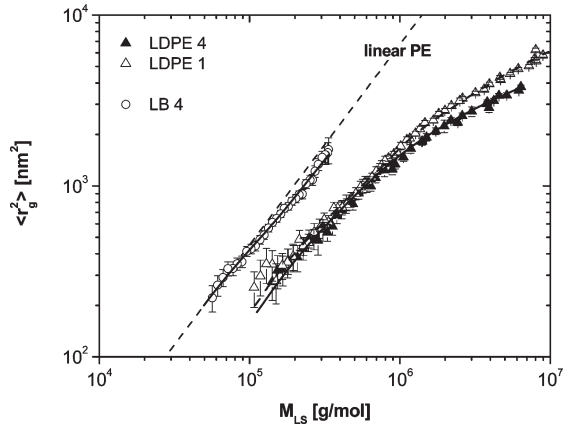

Figure 2. Expectation value of the square of the radius of gyration $\langle r_g^2 \rangle$ as a function of absolute molar mass for three different polyethylenes.[32]

The molar mass dependences of the radii of gyration of the products LB 1 and LB 4 are very similar. Therefore, only LB 4 is shown and discussed for reasons of clarity. For molar masses below about 150 000 g/mol, all measured radii lie on the line for the linear polyethylenes, whereas for high molar masses a slight coil contraction becomes visible. The coil contraction is an indication of few long-chain branches in the sample. In contrast, the LDPE resins exhibit a pronounced coil contraction over the whole range of molar masses confirming the high level of long-chain branching of the LDPE. In the high molar mass regime at molar masses above 10^6 g/mol, the LDPE 1 shows a somewhat weaker coil contraction. In addition, the LDPE 1 extends to higher molar masses than the LDPE 4.

Besides the qualitative assessment of the degree of branching obtained from GPC−MALLS, Table 1 contains another indicator for long-chain branching, which is derived from the measurements of the zero-shear rate viscosity η_0 (see next section on rheology). When correlating η_0 of linear polyethylenes with the absolute weight average molar mass M_w, for a broad range of molar masses a double-logarithmic slope of 3.4 to 3.6 was reported.[13,35,36] As has been shown by Gabriel and Münstedt,[10] Piel at al.[37] and others, the ratio of the measured zero-shear rate viscosity to the viscosity of a linear molecule of the same (absolute) weight average molar mass (scaling law by Stadler et al.[25]) allows for a discrimination of the different branching topographies. This ratio is called the zero shear-rate viscosity enhancement factor η_0/η_0^{lin}. A ratio around 1 stands for a linear molecule, values larger than 1 indicate a well-entangled molecule topography, with only few arms, while values below 1 are typical of a treelike branching structure of high branching functionality.

Rheology. *Linearity and Stationarity in Creep-Recovery Tests.* In a creep-recovery experiment a constant stress τ_0 is applied to the sample for a certain creep time $t = t_0$. At t_0 the stress τ_0 is set to zero and the recovery part of the experiment starts. The measured quantities are the strain γ as a function of creep time t and the recoverable strain γ_r as a function of the recovery time t_r.

The creep compliance $J(t)$ is defined as

$$J(t) = \frac{\gamma(t)}{\tau_0} \tag{2}$$

In the linear range of deformation, $J(t)$ is independent of the creep stress τ_0. The creep compliance consists of three parts, i.e.

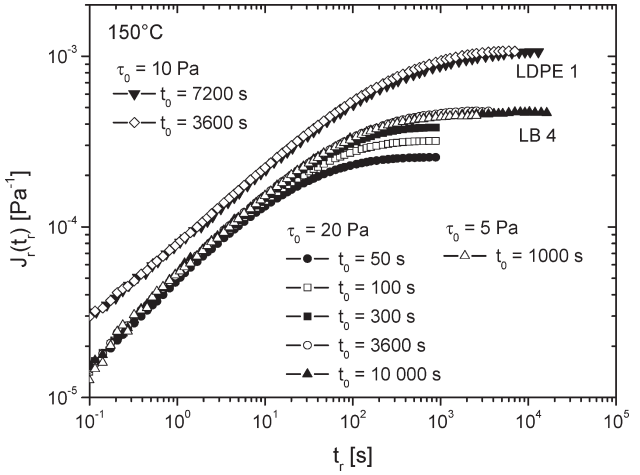

Figure 3. $J_r(t_r)$ for LB 4 and LDPE 1 at 150 °C measured at various shear stresses and different times t_0 of the preceding creep test.

$$J(t) = J_0 + \psi(t) + \frac{t}{\eta_0} \tag{3}$$

J_0 is the instantaneous elastic compliance, t/η_0 is the irreversible viscous term, and $\psi(t)$ is the viscoelastic part. η_0 is the zero shear-rate viscosity that can be determined from experiments conducted at stresses in the linear regime as

$$\eta_0 = \lim_{t \to \infty} \frac{t}{J(t)} \tag{4}$$

The recoverable compliance $J_r(t_r)$ is defined as

$$J_r(t_r, t_0) = \frac{\gamma_r(t_r, t_0)}{\tau_0} \tag{5}$$

and depends on the recovery time t_r as well as on the previous creep time t_0.[38] It can be decomposed into:

$$J_r(t_r, t_0) = J_0 + \psi(t_r, t_0) \tag{6}$$

For infinitely long creep and recovery times in the linear regime, the stationary value J_e^0 is obtained:

$$\lim_{\substack{t_r \to \infty \\ t_0 \to \infty}} J_r(t_0, t_r) = J_e^0 \tag{7}$$

In order to ensure that the linear terminal value of the steady-state compliance J_e^0 is obtained it has to be shown that its value is independent of the preceding creep time t_0, the recovery time t_r, and the applied stress τ_0. Figure 3 gives the dependence on creep time t_0 for LB 4 at a creep stress of 20 Pa applied for various times t_0 between 50 and 10 000 s. The curves for $J_r(t_r)$ merge at short recovery times. All of them show a stationary value, which increases with increasing creep time t_0. For the creep times of 3600 s and 10 000 s, however, the recoverable compliances $J_r(t_r)$ coincide, indicating that the highest possible recovery is reached. The creep-recovery at a stress of 5 Pa and a creep time of 1000 s is very similar with the curves after previous creep times of $t_0 = 3600$ s and 10 000 s at a stress of 20 Pa. This finding indicates that the measurements were performed in the linear regime and, therefore, J_e^0 is obtained. From these results the

experimental conditions of $\tau_0 = 20$ Pa and $t_0 = 4000$ s were chosen for the following experiments on this material. In addition, the stationarity for LDPE 1 is shown in Figure 3, too.

The proof for stationarity and linearity was conducted for all the samples. Thus, it was ensured that the linear and steady-state values are discussed in the following.

Temperature Dependence of Creep-Recovery Measurements

Linear mLLDPE. In Figure 4, the creep and the recoverable compliances of the two linear mLLDPE samples are plotted as a function of time. The creep compliances $J(t)$ of both materials reach the constant double logarithmic slope of one after about 10 s, even at the lowest measuring temperature of 130 °C indicating that after this time the steady state of creep was reached in good approximation. In this regime the zero-shear rate viscosities η_0 can be calculated from the creep curves. They are given in Table 1. The values of J_e^0 for both materials are very low.[39] They reflect the narrow molar mass distribution and the absence of long-chain branches (see also refs 16 and 21). The somewhat higher polydispersity of L 6−4 is not reflected by the linear steady state compliances,[40] which are listed for all temperatures measured in Table 2 and plotted in Figure 8 as a function of the inverse absolute temperature.[41]

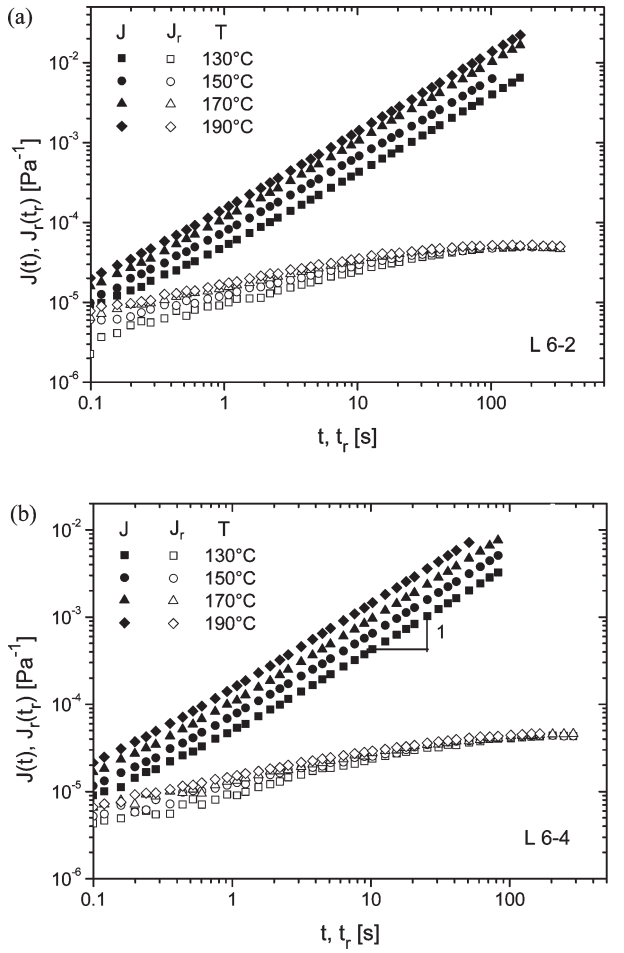

Figure 4. Creep compliance $J(t)$ and recoverable compliance $J_r(t_r)$ for mLLDPE (a) L 6−2 and (b) L 6−4 at various temperatures and stresses in the linear regime.

A closer look at the recoverable compliance $J_r(t_r)$ reveals that for both materials the steady state in the recovery experiment is already reached after about 100 s.

The linear steady-state compliances J_e^0 are independent of temperature for both samples. A detailed discussion concerning the temperature dependence of all materials will be given in the Discussion.

LCB-mLLDPE. The results of the creep-recovery measurements at four different temperatures for the two LCB-mLLDPE are given in Figure 5. Although the molar mass distributions are similar to those of the linear mLLDPE, the terminal relaxation times are much larger due to the long-chain branches. Thus, longer creep and recovery times are necessary to reach stationarity.

For short times when the viscous contribution to $J(t)$ is still negligible, $J_r(t_r)$ and $J(t)$ are nearly identical.[42] $J_r(t_r)$ start from a level about 1 decade higher compared to the linear mLLDPE and show a more pronounced time dependence than the linear mLLDPE. In contrast to the linear mLLDPE the curves of $J_r(t_r)$ for the different temperature cross each other and reach different stationary values J_e^0. Thus, J_e^0 is temperature dependent and increases with decreasing temperature. Explanations for this finding will be given later.

The values of J_e^0 for all products at all temperatures measured are listed in Table 2. It shows that for the long-chain branched mLLDPE the values for J_e^0 are more than 1 order of magnitude larger than for the two linear mLLDPE. J_e^0 is slightly higher for LB 1 than for LB 4. Taking the viscosity enhancement factor as the most sensitive tool for the effectiveness of the LCB into account, it has to be concluded that LB 4 is more branched than LB 1. The differences in branching are not reflected in the values of J_e^0. An explanation for these findings is given later in the discussion part.

LDPE. The recovery data of LDPE 1 and LDPE 4 are given in Figure 6.[43] The steady state could be reached in creep (not shown) and creep-recovery, although the necessary creep and recovery times are quite long (almost 30 000 s at 130 °C for LDPE 1). This is due to the high molar mass and the long-chain branching of LDPE 1. For LDPE 4 significantly lower creep and recovery times are required due to the lower molar mass M_w (Figure 6b). For LDPE 1 and LDPE 4 the linear steady-state compliances also show a decrease of J_e^0 with increasing temperature, which is weaker, however, compared to the LCB-mLLDPE resins, (see Figure 5a, Figure 5b, and Table 2).

Determination of Activation Energies. At long creep times the creep compliances $J(t)$ reach a constant double logarithmic slope of 1 in all the measurements performed, allowing

Table 2. J_e^0 [10^{-4} Pa^{-1}] Measured at Different Temperatures for the Materials Investigated[a] and Activation Energy E_a Determined from η_0

T [°C]	L 6−2	L 6−4	LB 1	LB 4	LDPE 1	LDPE 4
130	0.50 ± 0.01	0.45 ± 0.05	6.13 ± 0.55	5.14 ± 0.09	14.1 ± 0.1	11.7 ± 0.6
150	0.50 ± 0.02	0.46 ± 0.05	5.25 ± 0.08	4.50 ± 0.06	12.8 ± 0.6	11.0 ± 0.3
170	0.50 ± 0.02	0.45 ± 0.02	4.54 ± 0.08	3.98 ± 0.06	11.9 ± 0.4	10.3 ± 0.7
190	0.50 ± 0.02	0.46 ± 0.03	3.82 ± 0.22	3.55 ± 0.03	10.3 ± 0.9	9.8 ± 0.4
E_a [kJ/mol]	33.4 ± 1.1	33.6 ± 0.8	46.1 ± 1.0	48.9 ± 0.4	68.5 ± 1.1	64.0 ± 1.6

[a] The J_e^0 values in the table are averages of at least five independent measurements.

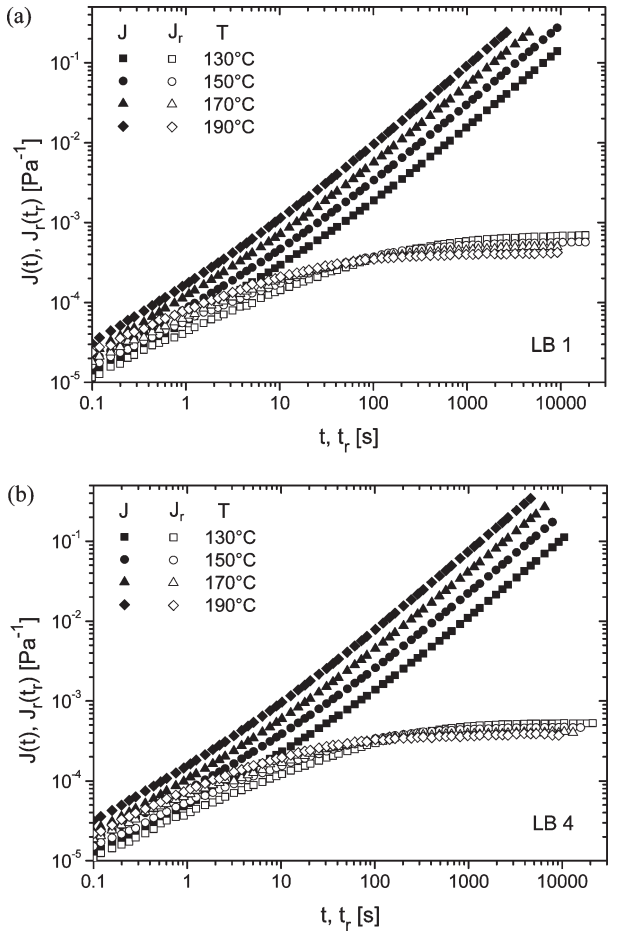

Figure 5. Creep compliance $J(t)$ and recoverable compliance $J_r(t_r)$ for LCB-mLLDPE (a) LB 1 and (b) LB 4 at various temperatures and stresses in the linear regime.

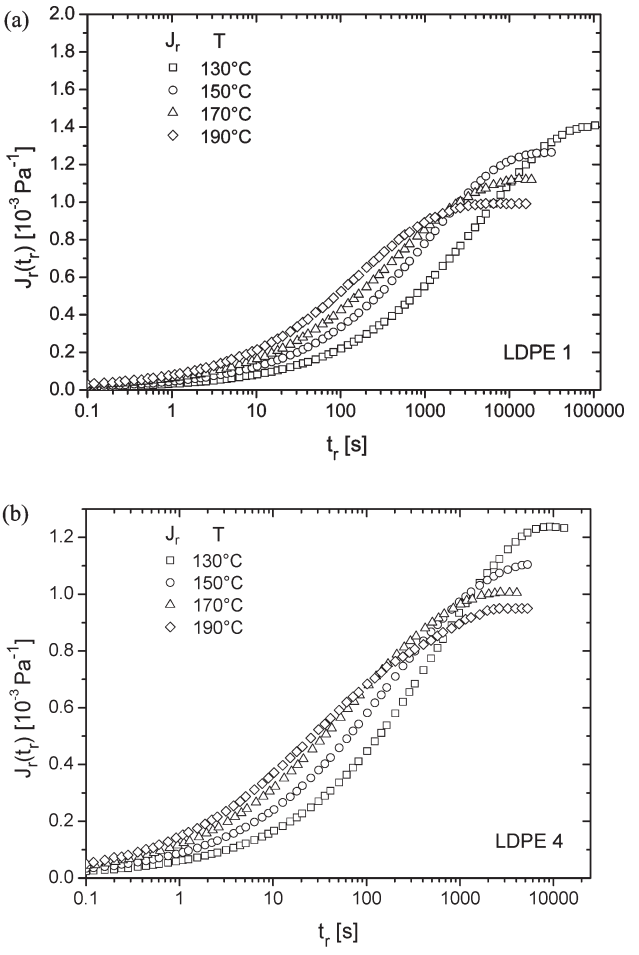

Figure 6. Recoverable compliances $J_r(t_r)$ for (a) LDPE 1 and (b) LDPE 4 at various temperatures and stresses in the linear regime.

the calculation of the zero-shear rate viscosities η_0 according to eq 4. The viscosities are presented in an Arrhenius-plot in Figure 7. As expected, a constant activation energy E_a is found for each sample from the slope of the linear fits to the data, which describe the experimental data very well.

The activation energies calculated from Figure 7 are listed in Table 2. Three categories can be distinguished. For the LDPE materials the highest activation energy is found, while the linear materials show the lowest values. The activation energies of the LCB-mLLDPE lie in-between. The E_a values determined are in good agreement with literature where activation energies in the range of 26−36 kJ/mol are reported for linear PE, 35−50 kJ/mol for LCB-mLLDPE, and around 60 kJ/mol for LDPE, respectively.[21,22,44,45]

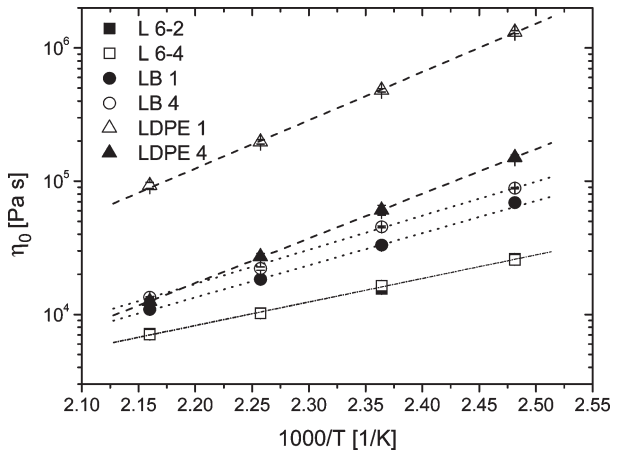

Figure 7. Arrhenius-plots of the zero-shear viscosities η_0 for all PE measured. The data of L 6−2 and L 6−4 cannot be distinguished.

Discussion

Increase of Elasticity by the Introduction of Long-Chain Branches. The LLDPE materials investigated allow a discussion of the influence of long-chain branches on the elastic properties as their molar-mass distributions are very similar.

J_e^0 of the LCB-mLLDPE LB 1 and LB 4 is about an order of magnitude higher compared to the linear mLLDPE L 6−2 and L 6−4 (Table 2). This increase in elasticity can solely be attributed to the long-chain branches. J_e^0 of LB 1 are slightly higher than those of LB 4 at all temperatures. A qualitative explanation can be derived using the results of SEC−MALLS and the findings of Graessley and Roovers[12] on star-branched polystyrenes of various functionalities. For the LCB-mLLDPE the radii of gyration (see Figure 2) come to lie on the line of the linear polyethylenes at low molar masses, while at higher molar masses the radii are somewhat smaller than those of the linear molecules. Therefore, it is concluded that these materials are mixtures of linear and long-chain branched molecules with a mostly starlike topography.[46] Graessley and Roovers observed for their star-branched polystyrenes of fixed functionality an increase of J_e^0 with molar mass. This increase is reflected in the

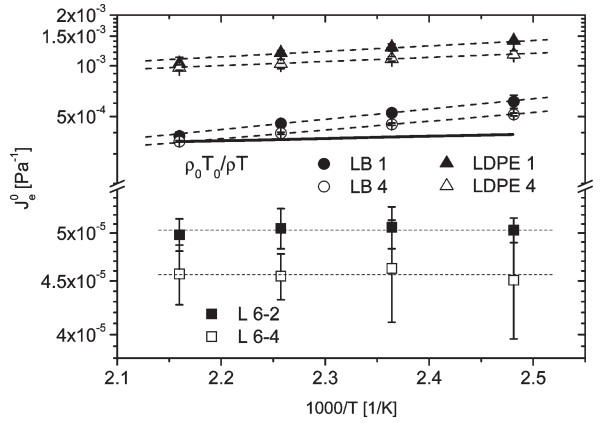

Figure 8. Logarithmic plot of the linear steady-state compliance J_e^0 as a function of the inverse absolute temperature for all PE investigated. The full line shows the density correction applied for LB 4 based on T_0 = 463 K.

description of the molar mass dependence of J_e^0 for stars given by Pearson and Helfland.[48]

$$J_e^0 = \nu' \frac{M_a}{M_e} \frac{1}{G_N^0} \tag{8}$$

In this equation, M_a is the molar mass of an arm of the star, M_e the entanglement molar mass ($M_e = 4/5\ \rho RT/G_N^0$), G_N^0 the modulus in the rubbery plateau, and ν' a constant prefactor in the order of 0.6. If the functionality of the star is fixed an increase of molar mass results in a growing molar mass of the arms M_a and finally in higher J_e^0. As in the case of LB 4 and LB 1 the weight average molar mass of LB 1 is about 10% higher (see Table 1), eq 8 would predict an increase in J_e^0 of the same order. The values in Table 2 show an increase of about 13% for LB 1 averaged over all temperatures. Therefore, the assumption of a constant average functionality of the branching structure in the LCB-mLLDPE seems to be reasonable, especially as the two materials are produced using the same technology.

For the LDPE the situation is more complex. Their J_e^0 is higher by a factor of 2 to 3 than those of the LCB-mLLDPE. In comparison to the LCB-mLLDPE two molecular parameters are changed for the LDPE. First, the molar mass distributions of the LDPE are much broader and have a high molecular weight tail. Both factors are known to increase the elasticity. For linear HDPE of a similar polydispersity even higher J_e^0 were reported.[21] Second, the coil contraction measured for the LDPE (cf. Figure 2) is much larger indicating a more branched structure. The increase in elasticity of LDPE 1 compared to LDPE 4 is presumably only caused by the broader molar mass distribution, as its coil contraction is similar to that of LDPE 4.

Temperature Dependence of the Linear Steady-State Compliance. In Figure 8, the linear steady-state compliance J_e^0 is plotted as a function of the inverse absolute temperature for all polyethylenes investigated. Three classes of temperature dependence can be distinguished.

For the linear mLLDPE the linear steady-state compliances J_e^0 are independent of temperature.

For the long-chain branched mLLDPE materials LB 1 and LB 4 and the two LDPE a distinct decrease of J_e^0 with temperature was found. The LCB-mLLDPE and LDPE investigated differ in their temperature dependence, however. J_e^0 of LDPE shows a distinctly weaker temperature dependence than that of the LCB-mLLDPE.[49] These findings have to be explained.

Assuming a temperature dependence of J_e^0 similar to that known from rubber elasticity the following equation should hold:[51]

$$J_e^0(T) = \frac{\rho_0 T_0}{\rho T} J_e^0(T_0) \tag{9}$$

According to this relation, a decrease of J_e^0 of about 15% is expected with increasing temperature in the temperature regime investigated assuming a coefficient of thermal expansion of 6×10^{-4} K^{-1} for the melt. In Figure 8 the change of J_e^0 caused by the temperature dependence of the entropic spring network is indicated for the material LB 4 as full line. The change in elasticity found in the experiments, however, is too pronounced as being able to be attributed to the temperature dependence originating from the model of rubber elasticity.

The temperature effect found cannot be related to a lack of stationarity, either. At a constant stress, the stationarity of the creep and the recovery experiments would be reached at shorter times for the higher temperatures. Thus, if nonstationarity would be an issue, at a distinct time the higher temperatures would result in higher values of J_e^0, and not in lower ones as found.

As the model of rubber elasticity and experimental conditions do not explain the different temperature dependences of J_e^0, differences of the molecular structure of the mLLDPE, LCB-mLLDPE, and LDPE may be the reason. As already pointed out in the previous chapter the LCB-mLLDPE have to be considered as blends of linear, starlike branched molecules and few more branched molecules, e.g., H-shaped species. Consequently, this behavior similar to a blend should also be visible in other rheological quantities, particularly, in the retardation and relaxation spectra. In agreement with literature for the investigated LCB-mLLDPE two main relaxation modes were found.[18,44,52,53] The one at shorter times was interpreted to correspond to the linear chains with low molar masses, while the longer one was assumed to be the consequence of the long-chain branched chains of higher relaxation or retardation times, respectively. In this interpretation, the linear molecules dominate the short retardation times and the branched molecules the longer ones. As an example, these assumptions are visualized in Figure 9 in which for two different temperatures the retardation spectra of the components as well as of the blend are shown. For the reason of simplicity, the same shape of the spectra is assumed for the linear and the LCB component. The spectrum of the blend was obtained by a linear superposition, which excludes any interaction between the two blend components.

As long-chain branched polyethylenes have a much higher activation energy than linear ones (cf. Table 2), a change of the temperature influences the mobility of the linear and branched molecules differently. Due to the higher activation energy of the long-chain branched molecules, their retardation times are lowered more by an increase in temperature than those of to the linear species (see Figure 9). Therefore, the assumed difference in retardation times between the linear and the long-chain branched molecules will decrease. As a consequence, J_e^0 given by

$$J_e^0 = \int_{-\infty}^{\infty} L(\tau)\, \mathrm{d}(\ln \tau) \tag{10}$$

will become temperature dependent.

Since the activation energy of the LCB molecules is larger than for the linear ones an increase in temperature makes the spread of the retardation spectrum axis more narrow

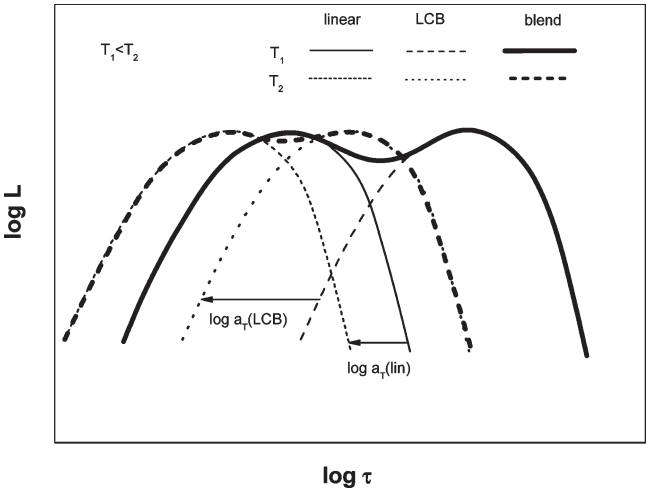

Figure 9. Schematic picture of the temperature dependence of the retardation spectrum L of a blend of linear and LCB molecules with different temperature dependencies.

(cf. Figure 9). Consequently, the integral according to eq 10 and, therefore, J_e^0 becomes smaller.

These considerations also allow the interpretation of the missing temperature dependence of J_e^0 of the linear mLLDPE. It is not unrealistic to assume that the linear mLLDPE consist of short-chain branched molecules only, which means that all molecules have the same temperature dependence. In such a case, a change in temperature leads to a shift of the whole spectrum by the same factor, leaving the shape of the spectrum and the integral of eq 10 unchanged.

The findings of a small temperature dependence of the two LDPE samples investigated can be explained as follows. In LDPE all molecules are long-chain branched. From the SEC−MALLS data (Figure 2) it can be concluded that the branching topography changes with molar mass. It is not too hypothetical to assume, however, that the differences in activation energies will be smaller compared to those between linear and LCB molecules.[2] As a consequence, the temperature dependence of J_e^0 will become less pronounced.

The temperature dependence of J_e^0 reflects the thermorheological complex behavior,[50] which is reported in the literature for LCB-mLLDPE and LDPE,[23,45] mostly from dynamic mechanical measurements. As in creep-recovery experiments the viscous properties are measured, too, the analysis of the temperature dependence of $J(t)$ would be of interest as well. At long measuring times, the viscous contributions dominate. When applying the shift-factors determined from the zero-shear rate viscosity to the $J(t)$ curves they should perfectly overlap in this regime. At short measuring times, however, the elastic contributions to $J(t)$ are significant, and thus, for the thermorheological complex materials, thermorheological complexity should be visible.

Conclusions

Comparing the linear steady-state shear compliances J_e^0 of the linear mLLDPE L 6−2 and the two LCB-mLLDPE which have a similar polydispersity index M_w/M_n conclusions with respect to the influence of LCB on the elasticity of the materials can be drawn. The introduction of mostly starlike and some H-shaped long-chain branches increases J_e^0 by an order of magnitude. For the LDPE resins of broad molar mass distributions and treelike branching topographies an increase of J_e^0 by about a factor of 20 with respect to the linear mLLDPE was measured. As two factors influencing the elasticity have been changed in the case of LDPE, a separation of the effect of molar mass distribution and of branching is not possible. However, it can be concluded that the starlike branching topography has a very pronounced influence on the elasticity even at low branching levels.

The linear steady-state compliance of linear mLLDPE has been shown to be independent of temperature whereas J_e^0 of LCB-mLLDPE increases with decreasing temperature. This experimental result not reported in the literature before cannot be explained by applying the usual correction factor $\rho_0 T_0/\rho T$ as the temperature effect is about four times stronger than predicted by this factor in the temperature regime investigated. The temperature dependence of J_e^0 for the LCB-mLLDPE can be explained by assuming that this material is a blend of linear and branched molecules (mostly three-arm stars, few H-shaped molecules), which possess different activation energies.[24] A change in temperature then produces different temperature shifts of the retardation times for the various species, resulting in a change of the shape of the retardation spectrum, which consequently leads to different values for J_e^0. This assumption is particularly strongly verified in case of the LCB-mLLDPE, for which the activation energy of the linear molecules is much lower than that of the long-chain branched species.

The LDPE show a temperature dependence of J_e^0 similar to the LCB-mLLDPE but the changes found are less pronounced. Therefore, following the arguments given above, processes with different activation energies are postulated for the LDPE, too. This assumption is supported by the dependence of the radii of gyration on M_w in Figure 2 which points to a higher effectivity of branches at larger molar masses than at smaller ones.

From these considerations, it was concluded that the temperature dependence of J_e^0 will be the stronger the larger the difference in the activation energies of the two (or more) species of different topography is.

Acknowledgment. The authors would like to thank the German Research Foundation (DFG) for the financial support of this work. The contributions of Mrs. I. Herzer (University Erlangen-Nürnberg) regarding the SEC−MALLS measurements are gratefully acknowledged.

References and Notes

(1) Plazek, D. J. In *Relaxations in Complex Systems*; Ngai, K. L., Wright, G. B., Eds.; Office of Naval Research: Arlington, VA, 1984; pp 83−109.
(2) Lohse, D. J.; Milner, S. T.; Fetters, L. J.; Xenidou, M.; Hadjichristidis, N.; Roovers, J.; Mendelson, R. A.; Garcia-Franco, C. A.; Lyon, M. K. *Macromolecules* **2002**, *35*, 3066–3075.
(3) Auhl, D.; Ramirez, J.; Likhtman, A. E.; McLeish, T. C. B.; Chambon, P.; Fernyhough, C. *J. Rheol.* **2008**, *52*, 801–835.
(4) Münstedt, H.; Katsikis, N.; Kaschta, J. *Macromolecules* **2008**, *41*, 9777–9783.
(5) Masuda, T.; Kitagawa, K.; Inoue, T.; Onogi, S. *Macromolecules* **1970**, *3*, 116–125.
(6) Orbon, S. J.; Plazek, D. J. *J. Polym. Sci., Polym. Phys. Ed.* **1979**, *17*, 1871–1890.
(7) Kurata, M. *Macromolecules* **1984**, *17*, 895–898.
(8) Pechhold, W.; v. Soden, W.; Stoll, B. *Makromol. Chem.* **1981**, *182*, 573–581.
(9) Graessley, W. W.; Struglinski, M. J. *Macromolecules* **1986**, *19*, 1754–1760.
(10) Gabriel, C.; Münstedt, H. *Rheol. Acta* **2002**, *41*, 232–244.
(11) Plazek, D. J.; Agarwal, P. K. *Proc. 7th Int. Congr. Rheol.* **1976**, 488–489.
(12) Graessley, W. W.; Roovers, J. *Macromolecules* **1979**, *12*, 959–965.
(13) Raju, V. R.; Rachapudy, H.; Graessley, W. W. *J. Polym. Sci., Part B: Polym. Phys.* **1979**, *17*, 1223–1235.
(14) Roovers, J.; Graessley, W. W. *Macromolecules* **1981**, *14*, 766–773.
(15) Gabriel, C.; Kaschta, J.; Münstedt, H. *Rheol. Acta* **1998**, *37*, 7–20.
(16) Gabriel, C.; Münstedt, H. *Rheol. Acta* **1999**, *38*, 393–403.
(17) Stadler, F. J.; Piel, C; Kaminsky, W.; Münstedt, H. *Macromol. Symp.* **2006**, *236*, 209–218.

(18) Stadler, F. J.; Piel, C.; Klimke, K.; Kaschta, J.; Parkinson, M.; Wilhelm, M.; Kaminsky, W.; Münstedt, H. *Macromolecules* **2006**, *39*, 1474–1482.
(19) Fujimoto, T.; Narukawa, H.; Nagasawa, M. *Macromolecules* **1970**, *3*, 57–64.
(20) Hepperle, J. *Einfluss der molekularen Struktur auf rheologische Eigenschaften von Polystyrol- und Polycarbonatschmelzen*; Shaker Verlag: Aachen, Germany, 2003.
(21) Gabriel, C. *Viskoelastisches Verhalten von Polyolefinschmelzen*; Shaker Verlag: Aachen, Germany, 2001.
(22) Vega, J. F.; Santamaria, A.; Munoz-Escalona, A.; Lafuente, P. *Macromolecules* **1998**, *31*, 3639–3647.
(23) Wood-Adams, P. M; Costeux, S. *Macromolecules* **2001**, *34*, 6281–6290.
(24) Stadler, F. J.; Kaschta, J.; Münstedt, H. *Macromolecules* **2008**, *41*, 1328–1333.
(25) Stadler, F. J.; Piel, C.; Kaschta, J.; Rulhoff, S.; Kaminsky, W.; Münstedt, H. *Rheol. Acta* **2006**, *45*, 755–764.
(26) Gabriel, C.; Kaschta, J. *Rheol. Acta* **1998**, *37*, 358–364.
(27) Plazek, D. J. J. *Polym. Sci., Part A-2: Polym. Phys.* **1968**, *6*, 621–638.
(28) Link, G.; Schwarzl, F. R. *Rheol. Acta* **1985**, *24*, 211–219.
(29) Stadler, F. J.; Münstedt, H. *J. Rheol.* **2008**, *52*, 697–712.
(30) To overcome the problem of the exact definition of the start of the recovery experiment creep breaking was used. It stops the rotation of the rotor at the programmed starting point of the recovery experiment by the application of a counter torque. This is necessary as the rotor would continue to rotate driven by its inertia even after the torque has been switched off. Thus, this technique allows an exact definition of the starting point of the recovery experiment even for rather low viscous fluids for which inertia effects become visible.
(31) Sun, T.; Brant, P.; Chance, R. R.; Graessley, W. W. *Macromolecules* **2001**, *34*, 6812–6820.
(32) The radii of gyration of the two LDPE have been truncated at molar masses below 100 000°g/mol as indications for nonideal separation in the GPC became visible. In this molar mass regime highly branched molecules of very high molar mass[33] and/or high molar mass stars[34] may elute together with low molar mass species making an interpretation with respect to structure impossible.
(33) Podzimek, S.; Vlcek, T.; Johann, C. *J. Appl. Polym. Sci.* **2001**, *81*, 1588–1594.
(34) Frater, D. J.; Mays, J. W.; Jackson, C. *J. Polym. Sci., Part B: Polym. Phys.* **1997**, *35*, 141–151.
(35) Jordens, K.; Wilkes, G. L.; Janzen, J.; Rohlfing, D. C.; Welch, M. B. *Polymer* **2000**, *41*, 7175–7192.
(36) Aguilar, M.; Vega, J.; Sanz, E.; Martinez-Salazar, J. *Polymer* **2001**, *43*, 9713–9721.
(37) Piel, C.; Stadler, F. J.; Kaschta, J.; Rulhoff, S.; Münstedt, H.; Kaminsky, W. *Macromol. Chem. Phys.* **2006**, *207*, 26–28.
(38) $\gamma_r(t_0,t_r)$ is defined as $\gamma(t_0) - \gamma(t_r)$; i.e., $J_r(t_0,t_r)$ is positive.
(39) The creep-recovery data show some waviness at short measuring times which is a consequence of the fact that the rheometer was operated closely to its limits.
(40) These findings may be due to a limited accuracy of the GPC.
(41) The values given in Figures 7 and 8 and in Table 2 are averages of at least five measurements on individual samples.
(42) For the linear mLLDPE the regime where $J(t)$ and $J_r(t_r)$ coincide lies at very short times which cannot be accessed by the experiment as viscous contributions are already visible at the shortest time of 0.1 s. Due to the extra viscous term in $J(t)$, $J_r(t_r)$ cannot be larger than $J(t)$.
(43) In order to make the differences in the temperature dependence of $J_r(t_r)$ clearly visible, the creep curves are omitted.
(44) Wood-Adams, P. M. *J. Rheol.* **2001**, *45*, 203–210.
(45) Mavridis, H.; Shroff, R. N. *Polym. Eng. Sci.* **1992**, *32*, 1778–1792.
(46) Costeux et al. assume that these materials may contain in addition a few H-shaped and more highly branched molecules.[47]
(47) Costeux, S.; Wood-Adams, P.; Beigzadeh, D. *Macromolecules* **2002**, *35*, 2514–2528.
(48) Pearson, D. S.; Helfand, E. *Macromolecules* **1984**, *17*, 888–895.
(49) The plot of J_e^0 as a function of the inverse absolute temperature would allow a determination of "apparent" activation energies.[50] However, the molecular process responsible for the vertical shift is yet unclear. Therefore, no "apparent" activation energies are reported.
(50) Kessner, U.; Kaschta, J.; Münstedt, H. *J. Rheol.* **2009**, in press.
(51) Ferry, J. D. *J. Am. Chem. Soc.* **1950**, *72*, 3746–3752.
(52) Malmberg, A.; Gabriel, C.; Steffl, T.; Münstedt, H.; Löfgren, B. *Macromolecules* **2002**, *35*, 1038–1048.
(53) Gabriel, C.; Kokko, E.; Löfgren, B.; Seppälä, J.; Münstedt, H. *Polymer* **2002**, *43*, 6383–6390.